International Journal of Applied Earth Observation and Geoinformation 31 (2014) 25–36

Contents lists available at ScienceDirect

International Journal of Applied Earth Observation and Geoinformation

journal homepage: www.elsevier.com/locate/jag

Using Landsat Thematic Mapper records to map land cover change and the impacts of reforestation programmes in the borderlands of southeast Yunnan, China: 1990–2010

Jialong Zhang[a,*], Thi-Thanh-Hiên Pham[b], Margaret Kalacska[c], Sarah Turner[c]

[a] Faculty of Forestry, Southwest Forestry University, 300 Bailongsi, Kunming, Yunnan 650224, PR China
[b] Departement d'études urbaines et touristiques, Université du Québec à Montréal, Montréal, Canada
[c] Department of Geography, McGill University, Montréal, Canada

ARTICLE INFO

Article history:
Received 16 October 2013
Accepted 21 January 2014

Keywords:
Land cover monitoring
Landsat TM
Support vector machines
Reforestation
Yunnan
China

ABSTRACT

At the beginning of the new millennium, after a severe drought and destructive floods along the Yangtze River, the Chinese government implemented two large ecological rehabilitation and reforestation projects: the Natural Forest Protection Programme and the Sloping Land Conversion Programme. Using Landsat data from a decade before, during and after the inception of these programmes, we analyze their impacts along with other policies on land use, land cover change (LULCC) in southwest China. Our goal is to quantify the predominant land cover changes in four borderland counties, home to tens of thousands of ethnic minority individuals. We do this in three time stages (1990, 2000 and 2010). We use support vector machines as well as a transition matrix to monitor the land cover changes. The land cover classifications resulted in an overall accuracy and Kappa coefficient for forested area and cropland of respectively 91% (2% confidence interval) and 0.87. Our results suggest that the total forested area observed increased 3% over this 20-year period, while cropland decreased slightly (0.1%). However, these changes varied over specific time periods: forested area decreased between 1990 and 2000 and then increased between 2000 and 2010. In contrast, cropland increased and then decreased. These results suggest the important impacts of reforestation programmes that have accelerated a land cover transition in this region. We also found large changes in LULC occurring around fast growing urban areas, with changes in these peri-urban zones occurring faster to the east than west. This suggests that differences in socioeconomic conditions and specific local and regional policies have influenced the rates of forest, cropland and urban net changes, disturbances and net transitions. While it appears that a combination of economic growth and forest protection in this region over the past 20 years has been fairly successful, threats like drought, other extreme weather events and land degradation remain.

1. Introduction

Globally, land use change – including deforestation, agricultural expansion and urbanization – are occurring at an unprecedented pace, with major implications for the environment including climate change, land degradation, water depletion, as well as for human well-being, for instance disease, food provision and security (Foley et al., 2005; Jakobsen et al., 2007; Vanwambeke et al., 2007). Changes in forest cover are particularly important because of the ability of forests to sequester atmospheric carbon (Bonan, 2008), while changes in croplands are critical to food production and food security. While there is an important body of research on land use land cover change (LULCC) covering a number of geographic regions (see among others Chowdhury and Turner, 2006; Gray et al., 2008; Muller and Munroe, 2008), little is known about LULCC in the diverse and rugged borderlands of southwest China, home to tens of thousands of ethnic minority individuals.

Among the various sources of multispectral remotely sensed imagery, Landsat data constitute the longest record, making it possible to monitor land cover change using medium spatial resolution imagery with a high temporal frequency (Woodcock et al., 2008; Sexton et al., 2013). However, the extraction of detailed land cover classes from multispectral imagery increases the classification difficulty in heterogeneous areas because of the spectral similarity of some land cover types (Song et al., 2005). Spatial semantic characteristics (SSC) deal with spatial relationships (Ton et al., 1991) (e.g., proximity, connectivity, orientation) among various objects in order to minimize classification errors. For example, cropland is usually near a farmer's residence, or along a river, while a

* Corresponding author. Tel.: +86 871 63863022.
E-mail address: jialongzhang@swfu.edu.cn (J. Zhang).

0303-2434/$ – see front matter © 2014 Elsevier B.V. All rights reserved.
http://dx.doi.org/10.1016/j.jag.2014.01.006

water body cannot be on a steep slope. In this manner SSC guide the selection of training points to improve detailed land cover classifications.

The aim of our study is to analyze LULCC in Honghe and Wenshan Prefectures, in the southeast of Yunnan province, from 1990 to 2010 by using SSC with Landsat Thematic Mapper (TM) imagery. Specifically, we focus on crop and forest classes to examine the direct impacts of state reforestation programmes on local LULCC. Due to a severe drought in 1997 and destructive floods along the Yangtze River in 1998, the Chinese government created two large ecological rehabilitation projects (Xu et al., 2006): the Natural Forest Protection Programme (NFCP) established in 1998; and the Sloping Land Conversion Programme established in 1999 and effective from 2003 (SLCP, also known as the Grain to Green Programme and Conversion of Cropland to Forest and Grassland) (Liu et al., 2008). The objective of the SLCP was to convert or return agricultural croplands on steep slopes to forests or grasslands to promote reforestation and reduce runoff (Xu et al., 2004). As a result of these two programmes, forest cover in other parts of Yunnan has been reported to have increased, but with negative impacts on the livelihoods of communities living in mountainous regions (Weyerhaeuser et al., 2005). Concurrently, the China Western Development policy was also implemented from 2000 bringing new infrastructure, economic investment and plans to improve the welfare of the region's population through accelerated urbanization and other land cover changes (Lai, 2002).

Due to limited historical ground truthing data and the diverse land use types in this area, using Landsat imagery to accurately map land cover change is challenging, especially as land cover types are spatially and temporally diverse. In this paper, our specific objectives are:

- To quantify the changes of the predominant land cover classes from 1990 to 2010. This temporal period includes the decade before the reforestation programmes (1990–2000), and the decade after the reforestation programmes were initiated (2000–2010).
- To compare the overall forest and cropland change in the study area of four of Yunnan province's borderland counties, namely Jinping, Hekou, Maguan and Malipo.
- To analyze spatial and temporal changes in crop-land and forest with regards to the reforestation programmes, topography and socioeconomic factors.

2. Study area

Our study area in the Sino-Vietnamese borderlands encompasses Jinping and Hekou counties in Honghe Hani and Yi Autonomous Prefecture (commonly called Honghe prefecture), and Maguan and Malipo counties in Wenshan Zhuang and Miao Autonomous Prefecture (Wenshan prefecture), in southeast Yunnan (Fig. 1). These four counties cover 9851 km^2, with elevations ranging from 32 m to 3038 m, and an average temperature in 2008 of 19 °C. The Red River (Pinyin: *Hong He*), which begins in the mountains of northwest Yunnan, cuts across our study area before entering Vietnam and finally reaching the South China Sea. This 900 km long river fault forms complex valleys and steep mountains across our study area.

This borderland region is home to Miao, Yao, Yi, Dai, Zhuang, Buyi, Lahu, Gelao, and Menggu ethnic minorities, as well as Han Chinese. Jingping county has a population of 356,227, with the largest ethnic minority group being the Hani (26%), with 14% Han. Hekou county has a population of 104,609, of whom 23% are Yao, with 38% Han; while Malipo's population is 277,960, with 18% Miao and 58% Han. Finally, Maguan's population is 367,507, with 22% Miao and 49% Han (Yunnan Census Office and Statistical Bureau of Yunnan Provincial Government, 2012). Our study area has high levels of poverty compared with other parts of China, despite recent poverty alleviation policies and abundant natural resources. The push for local farmer involvement in cash-crops has been fairly persistent over the past twenty years, especially as a feature of China's Western Development Programme. As a result, ethnic minority farmer involvement in tobacco, banana and other cash crops has risen quickly (Peng, 1996; Singh, 2002; Goodman, 2004; Wang, 2012; Yang, 2012).

From west to east, Jinping county is known in China for the Fen Shui Ling National Natural Reserve as well as for varieties of non-ferrous metals. In the highest mountain ranges cardamom (*Amomum tsaoko*, Pinyin: *Caoguo*) is cultivated, while below 1600 m there are tree plantations and other cash crops (Wu et al., 2010). Hekou country has tropical seasonal rain forest and extensive cash crops including rubber, banana, pineapple and coffee (Local Chronicle Office of Honghe Prefecture, 2009). Maguan county includes rice and tobacco plantations, as well as *A. tsaoko* grown under forest plantation canopy, while Malipo county has a karst limestone environment, with maize as the staple crop, grown in shallow pockets of soil among rock (Yang et al., 2010; Local Chronicle Office of Wenshan Prefecture, 2011).

3. Methods

3.1. General approach

Using Landsat TM images and a SSC combined strategy for selecting training points, we mapped LULCC and analyzed its correlations with socioeconomic factors in these borderlands from 1990 to 2010. We concentrated on the classification of eight land cover types (closed canopy forest, open canopy forest, shrubs, water bodies, cropland, built up area, bare land, shade and cloud) and the transition between forest and cropland. We employed a Support Vector Machine (SVM) classifier using multi-temporal Landsat TM images from three different time periods (1990, 2000, 2010) to quantify LULCC during two intervals (1990–2000, 2000–2010) in response to the reforestation programmes. We assessed the relationships between land cover classes and socioeconomic factors using Pearson correlation analysis to enhance the interpretations of the main causal factors of land cover change.

3.2. Satellite images and image pre-processing

Two Landsat images footprints (path/row 129/044 and 128/044) covered our study area and we used a total of eight images. The Landsat images were downloaded from the USGS (http://glovis.usgs.gov/). We selected images with the least cloud cover (primarily winter images). Six TM images were selected for land cover classification acquired on 01/09/92, 26/11/00, 03/11/09 (Path: 129, Row: 44) and 04/08/90, 03/11/00, 15/01/10 (Path:128, Row:44). One ETM+ (Path: 129, Row:44) acquired 15/09/00 and another TM (Path:128, Row:44) acquired on 28/04/95 were used to help eliminate the cloud cover during post classification.

We converted the image DN values to radiance following Chander et al. (2009). Then we used the FLAASH module in ENVI 4.7 (Berk et al., 1998; Matthew et al., 2000) to atmospherically correct the images (Atmospheric model: Tropical; Aerosol Model: Rural; Aerosol Retrieval: 2-Band (KT); Visibility: 25–40 km). While we did not include a topographic correction, we added shade classes to the classification, then merged some of them with the neighbouring sunlit categories we had after image classification.

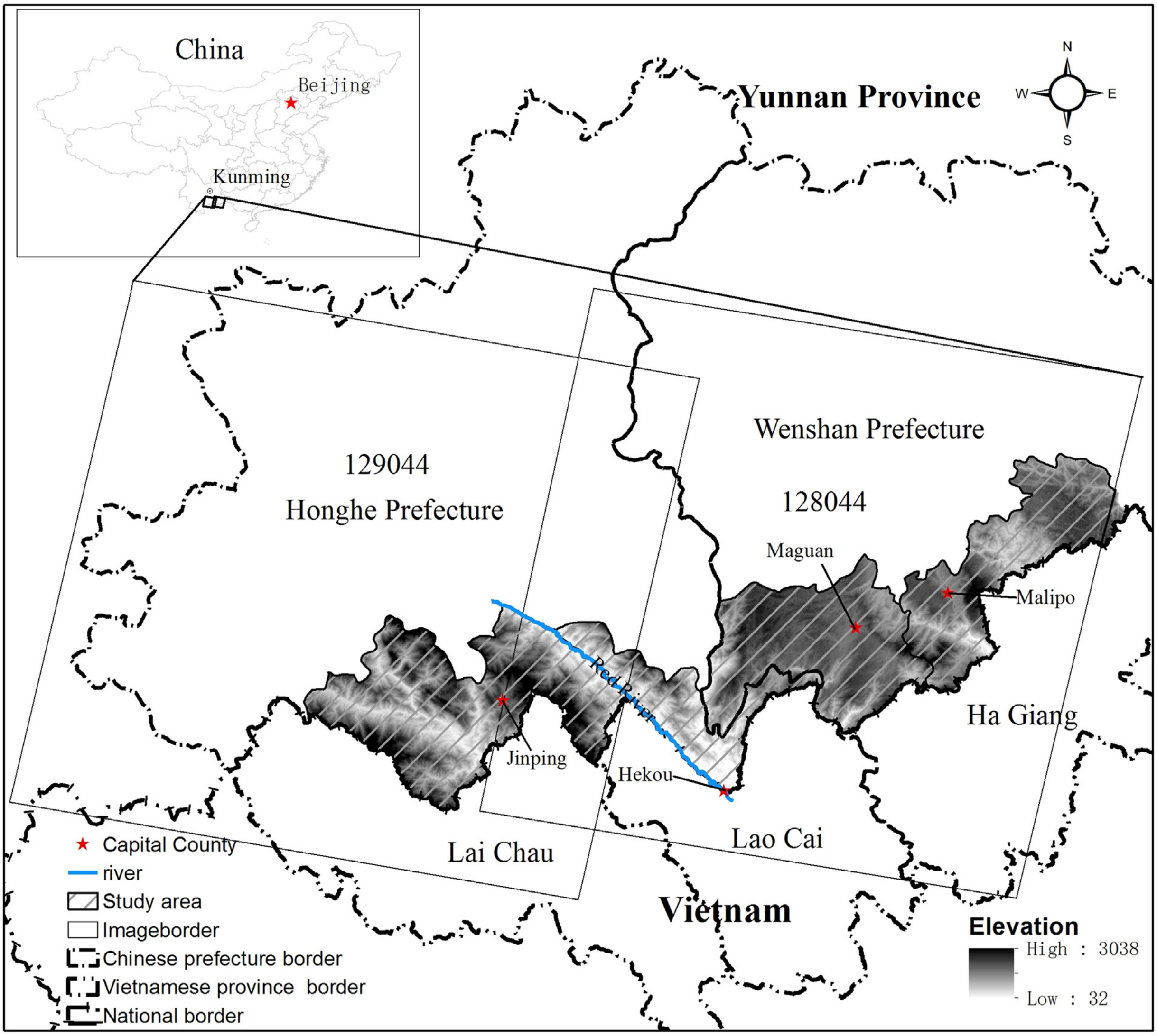

Fig. 1. Location of study area: Jinping and Hekou counties in Honghe prefecture; and Maguan, and Malipo counties in Wenshan Prefectures, Yunnan, China.

3.3. Training data

Data for training were collected from fieldwork, a government issued 2009 land use map and Google Earth. Fieldwork was conducted in March 2013, at locations across the study area from Jinping in the west to Malipo in the east, in order to capture the variations of the seven land use/cover types on the ground. In areas where there was no significant change in relief or land cover, one GPS point was taken every 10 km. In heterogeneous landscapes, GPS points for the two to three most dominant land cover types within each 10 km were taken. At each GPS point, four photographs in the four cardinal directions were also taken. The GPS error ranged from 3 to 6 m. This ground truth data was complemented by ethnographic fieldwork undertaken in the region in June 2010, including interviews with ethnic minority farmers regarding their livelihoods and land use changes.

Another source of ground truth data was the Hekou 2009 land use map (geo-registration error approximately 10 m), which had been validated during the 2007–2009 Chinese national second land use investigation. We used the polygons of the land use map as a base map to collect additional points. As a third source of data, 1600 points were collected from Google Earth for the 2010 time period. Lastly, we used SSC combined with NDVI and band composites to reduce the uncertainty of heterogeneous classes to select training points for all the images. More specifically, we defined semantic rules (i.e. SSC strategies) to help separate pixels having similar spectral values on the Landsat images, which could belong to at least two different classes. By ‘semantic’ we mean a human evaluation of a group of pixels in order to decide which land cover they could be on the ground, based on size of the group of the pixels and its proximity to other land cover types. For example, to separate pixels that could belong to ‘sand’ and ‘built-up area’, we assigned pixels to ‘sand’ if they were close to water bodies and concentrated in small areas, while those that concentrated in large zones were assigned to ‘built-up area’. To separate pixels that could belong to either ‘shrubs’ or ‘cropland’, those that were close to roads were assigned to be ‘cropland’. Such rules were developed based on our field observations.

Table 1 shows the land cover classification scheme, based on the Chinese Second Land Investigation—National standard of current land use classification GB T21010-2007, as well as the strategy of collecting training points.

Table 1
Land cover classification scheme and strategy of selecting training points.

Categories	Definition	RGB 4/3/2	RGB 7/4/2	RGB 3/2/1	Ground picture
1: Closed canopy forest	Old and dense trees, greater than 5 m tall and 50% cover, NDVI ≥0.7	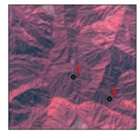	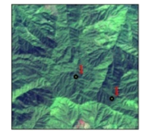	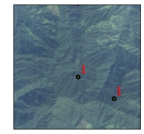	
2: Open canopy forest	Less dense, often re-growth trees/orchards, greater than 2 m tall and 30% cover, NDVI ≥0.5 and < 0.7	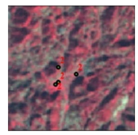	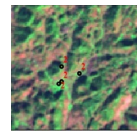		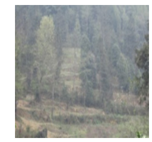
3: Shrubs	Open grass mixed with small shrubs, less than 3 m tall, NDVI ≥0.3 and <0.5		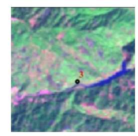		
4: Water	Rivers, lakes that remain throughout the year	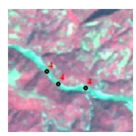	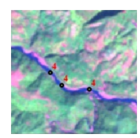		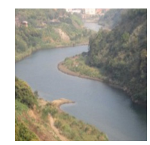
5: Cropland	Dry land or terraces, irrigated land	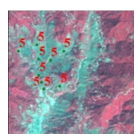	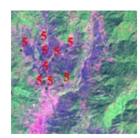		
6 Built-up area	The capital of the county	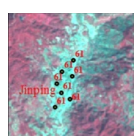	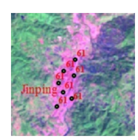	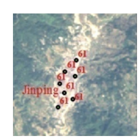	
6.1 Head county					
6.2 Town and village	Smaller urban areas than the capital	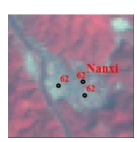	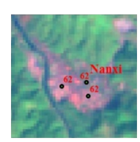	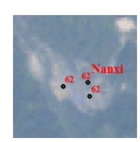	
6.3 Road		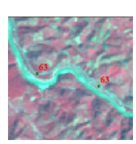	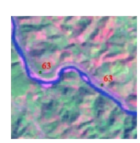		
6.4 Special buildings	Water conservation facilities	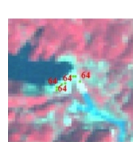	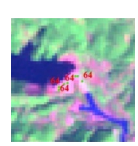	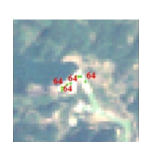	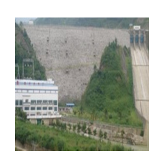
7.1 Shade: Where there is no sun illumination in the rugged high mountains; 7.2 clouds; 8.4 error pixels					
8 Bare land	No vegetation cover	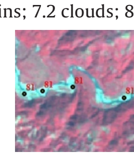		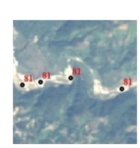	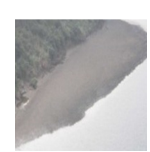
8.1 Sand					

Table 1 (*Continued*)

Categories	Definition	RGB 4/3/2	RGB 7/4/2	RGB 3/2/1	Ground picture
8.2 Bare soil		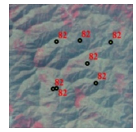	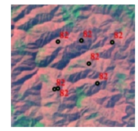	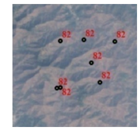	
8.3 Karst stone		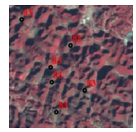	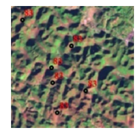	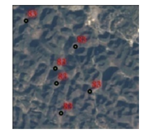	

Notes: for linear classes (e.g. river, road), training points (annotated on maps) were arranged with intervals of 5–10 km; for classes with large areas (e.g. forest), points were randomly distributed; for very diverse areas (e.g. around the head town of a county), points were more densely clustered; for cropland mixed with shrubs or less dense forest, points were arranged to cover each land cover type.

Table 2
The number of training points and polygons for each class.

Code	Land cover classes	Points	Polygons	Area ($100 \times m^2$)
1	Closed canopy forest	618	53	98,109
2	Open canopy forest	463	34	38,007
3	Shrubs	1108	40	25,110
4	Water bodies	961	0	8649
5	Cropland	1775	61	48,555
6	Built-up area	525	13	21,321
7.1	Shade	174	0	1566
7.2	Cloud	173	0	1557
8.1	Sand	88	3	1287
8.2	Bare soil	105	0	945
8.3	Karst stone	297	13	6867
8.4	Error pixel of image itself	95	0	855
	Total	6382	217	252,828

3.4. *Land cover classification*

The separability of the classes was evaluated for each pair of classes with the Jeffries-Matusita (J-M) distance (Richards and Jia, 1999). If the J-M distance values were low, we checked the validity of the points and for some classes added additional training points. For the closed canopy forest and cropland classes, small polygons were digitized in the images to capture the diversity of the spectra of these classes. In total, 6382 training points and 217 polygons were used, approximately 0.5 percent of the training points for the 2010 classification were from Google Earth (Table 2).

We used a Support Vector Machines (SVM) classifier in ENVI 5.0 to classify our images using the bands 1–5 and 7. This separated the classes with a multi-dimensional feature surface (Foody and Mathur, 2004) that maximizes the margin between the classes.

Accuracy assessment was performed in five steps. The first step was to determine the sampling size from Eq. (1) (Tortora, 1978; Congalton, 2009).

$$n = \frac{B(1-\pi_i)}{\pi_i b_i^2} \tag{1}$$

where B is determined from a chi-square table with 1° of freedom and $1-\alpha/k$. π_i is the proportion of ith category/class. K is the number of categories/classes in the classification (in this case $k = 8$). The desired confidence level is 95%, so here $\alpha = 0.05$. Only sample size calculation required is for the π_i closest to 50%, the value of π_i was based on the knowledge of the classification. The total sampling size was 681, 623 and 646 for the 1990, 2000 and 2010 classifications respectively.

The second step was to select the reference data. A new random set of points was created in ArcGIS 10 to ensure independence from the training samples. For the 2010 image, the points were labelled from Google Earth. Around 10 points were referenced from the images themselves where there was cloud on Google images. For the older images, we used the combined SSC strategy to label the points. The next step was to calculate error matrices to derive producer's accuracy (PA, errors of omission) and user's accuracy (UA, errors of commission), overall accuracy (OA) and the kappa statistic (Congalton, 1991; Foody, 2002). Fourth, confidence intervals for error matrices were computed according to Card (1982), to correct bias by incorporating estimated marginal proportions and from asymptotic variances. The estimated error matrix was computed with individual estimated cell probabilities calculated as (Eq. (2)) (Stehman and Czaplewski, 1998; Stehman, 2004):

$$\hat{p}_{ij} = \left(\frac{N_{i.}}{N}\right)\left(\frac{n_{ij}}{n_{i.}}\right) \tag{2}$$

where $N_{i.}$ is the number of pixels in the entire map of class i, N is the number of pixels of the entire map, $n_{i.}$ is the number of pixels in the sample of class i, n_{ij} is the sample count in row i and column j.

The next step was to correct the three accuracy rates by using the following equations:

$$\hat{p}_{PA} = \frac{\hat{p}_{ij}}{p_{.j}} \tag{3}$$

$$\hat{p}_{UA} = \frac{\hat{p}_{ij}}{p_{i.}} \tag{4}$$

$$\hat{p}_{OA} = \sum \hat{p}_{kk} \tag{5}$$

where $\hat{p}_{PA}$ is the corrected producer's accuracy, $\hat{p}_{UA}$ is the corrected user's accuracy and $\hat{p}_{OA}$ is the corrected overall accuracy. The estimated maginal proportion $\hat{p}_{.j}$ in reference land-cover class j is calculated by summing the $\hat{p}_{ij}$ in column j of the estimated error matrix. The estimated maginal proportions $\hat{p}_{i.}$ in classified land-cover class j is calculated by summing the $\hat{p}_{ij}$ in row i of the estimated error matrix. $\hat{p}_{kk}$ are diagonal values of the estimated error matrix (Stehman and Czaplewski, 1998). The confidence intervals for PA, UA and OA were then calculated from the corrected values by adding or subtracting variance values (Congalton, 2009).

Finally, the classified area was adjusted to correct the estimate error to quantify the sampling variability (Olofsson et al., 2013). The estimated stand error of the estimated area proportion is (Eq. (6)):

$$S(\hat{p}_{.j}) = \sqrt{\sum_{i=1}^{k} \pi_i^2 \frac{n_{ij}/n_{i.}(1-(n_{ij}/n_{i.}))}{n_{i.}-1}} \tag{6}$$

Table 3
Corrected producer and user accuracy, overall accuracy, Kappa coefficient, unbiased estimator of area and confidence intervals (CI) for specific classes.

Time stage	Class	Corrected PA	±CI (%)	Corrected UA	±CI (%)	Unbiased estimator of area (ha)	$\pm 2S(\hat{p}_{.j})$ (%)
1990	Closed canopy forest	95.1%	3.1	92.6%	2.1	274,395	1.4
	Open canopy forest	93.2%	5.7	93.2%	2.0	113,869	1.0
	Shrubs	93.0%	3.2	95.5%	1.7	345,542	1.5
	Cropland	94.9%	3.9	94.2%	1.9	184,761	1.1
	Overall accuracy	94.0%	1.6				
	Kappa Coefficient	91.7%					
2000	Closed canopy forest	96.4%	2.9	91.4%	2.4	270,414	1.5
	Open canopy forest	90.3%	5.1	91.5%	2.4	215,353	1.7
	Shrubs	83.8%	6.3	95.4%	1.8	198,873	2.1
	Cropland	94.8%	3.7	85.0%	3.0	234,057	2.0
	Overall accuracy	91.2%	2.3				
	Kappa Coefficient	88.1%					
2010	Closed canopy forest	95.7%	3.2	86.9%	2.9	276,430	2.0
	Open canopy forest	77.6%	7.1	85.1%	3.1	187,530	2.5
	Shrubs	86.9%	4.8	90.6%	2.5	295,350	2.5
	Cropland	84.8%	6.3	84.8%	3.1	184,994	2.5
	Overall accuracy	87.7%	2.5				
	Kappa Coefficient	82.1%					

and an approximate 95% confidence interval for the area of class j (Eq. (7)),

$$A_{total} \times \hat{p}_{.j} \pm 2 \times S(\hat{p}_{.j}) \quad (7)$$

For the post classification, we first merged shade classes into the sunlit ones when it was clear which class they belonged to. In cases where it was not known by visual evaluation what the land cover was in the shaded areas, they were kept separate.

3.5. Analysis of land cover change

To highlight the complexity of LULCC and gain a better understanding of forest and cropland transitions in relation to the forestation programmes, we undertook our analysis in three ways. First, we summarized areas of all classes during the three time stages. To account for the proportions of change of consistent classes, we integrated the second grade classes into the first grade categories (e.g. second grade 6.1–6.4 classes were all integrated into first grade 6). Then we quantified the proportions of land cover classification of the whole area and county level in the time stages of 1990, 2000 and 2010.

Second, we calculated the land cover relative net change (RNC) of the whole time period following (Kuemmerle et al., 2009) (Eq. (8)):

$$\mathrm{RNC} = \left(\frac{\mathrm{LC}_j}{\mathrm{LC}_{j-1}}\right) * 100 \quad (8)$$

with LC_j, LC_{j-1} as land cover area in km^2 at the end, beginning of the two time periods at two different levels: county and township (a county comprises a number of township units). Also, at the entire study area level we calculated annual land cover disturbance rates (LCDR) for each time period following (Baumann et al., 2012; Brandt et al., 2012) (Eq. (9)):

$$\mathrm{LCDR}_j = \left(\frac{D_j}{\mathrm{LCB}_j}\right) * 100/\mathrm{t} \quad (9)$$

where D_j is the overall area of the land cover loss during the analyzed time period j, LCB_j is the land cover at the beginning of the same time period, and t is the number of years in time period j.

Finally, to better understand FA and cropland gain or loss, we overlaid the three time-step land cover maps to quantitatively estimate the net transition rate (NTR) of FA and cropland in each time period using the cross-tabulation matrices based on land cover classification (Pontius, 2002; Takada et al., 2010) (Eq. (10)).

$$\mathrm{NTR} = \frac{(\mathrm{LC_{Ai}} + \mathrm{LC_{Bj \to Aj}} - \mathrm{LC_{Aj \to Bj}})}{\mathrm{LC_{Ai}}} * 100 \quad (10)$$

where $\mathrm{LC_{Ai}}$ is the area of the land cover pattern A that remained unchanged in time period i (1990 or 2000), $\mathrm{LC_{Bj \to Aj}}$ is transition area of land cover from pattern B to pattern A in time period j (2000 or 2010), and $\mathrm{LC_{Aj \to Bj}}$ is transition area of land cover from pattern A to pattern B in time period j.

The township boundaries were geo-referenced to the boundaries of the counties and then digitized from the newest township boundary map (Baidu.com). To understand the anthropogenic influence on the predominant land cover changes, we examined the population density at the township level and collected socioeconomic variables by county. These included total population, population of ethnic minorities, per capita income, and per capita net income of rural households from 1990 to 2010 at 2 years intervals. These data were gathered from the Yunnan Statistical Yearbook from 1990 to 2010, Yunnan census data for 1990, 2000, 2010, and population census of China 2000. Population at the township level in 2000 was acquired from the official website of the State statistics bureau and aggregated to the newest units based on the Adjustment of Chinese administrative divisions (http://www.xzqh.org/). To quantify the degree of conversion between cropland and FA land, we categorized slope into five grades: ≤2°, 2.1–6°, 6.1–15°, 15.1–25°, >25.1°. Finally, in order to analyze relationships between land cover change and socio-economic data, qualitative evaluations were conducted.

4. Results

4.1. Land cover classifications

Our classification resulted in an average overall accuracy of 90.9% (2.1% confidence interval) and kappa coefficient of 0.873 for all images (Table 3). We grouped closed canopy forest, open canopy forest, and shrubs together as forest area (FA) due to the reforestation programmes' focus of returning cropland to forest and shrubs. The class of closed canopy forest has the highest corrected producer's accuracy of 96.4% (maximum 99.3%, minimum 93.4%). The classes in 2010 have moderately lower accuracy than the other two stages, possibly because of some of the referenced points being near the pixel edges. There were around ±2% proportion

Table 4
Uncorrected producer and user accuracy of water bodies, built-up areas and bare land.

Images	Accuracy (%)	Water bodies	Built-up areas	Bare land
2009, Path:129, Row:44	PA	81.25	63.68	30.32
	UA	95.12	73.82	87.5
2010, Path:128 Row:44	PA	71.43	49.13	63.3
	UA	77.98	69.33	66.5
2000, Path:129, Row:44	PA	23.85	90.38	96.36
	UA	100	88.68	86.89
2000, Path:128 Row:44	PA	72.17	91.59	38.15
	UA	84.69	95.58	94.87
1992, Path:129, Row:44	PA	75	60	66.67
	UA	78.46	90	80
1990, Path:128 Row:44	PA	63.18	89.12	89.9
	UA	85.8	94.59	90.82

discrepancies of the four predominant classes between the classified and the calculated true marginal proportions, but they were less than ±2% for the FA and cropland. The cropland in 1990, 2000 and 2010 increased from 184,761 (±10,922 ha) to 234,057 (±19,305 ha) and then decreased to 184, 994 (±24,360 ha) (95% confidence interval), whereas the land cover change to FA showed the opposite trend.

For built-up areas, water bodies and bare land, we only computed uncorrected producer and user accuracy obtained from the six image classification (Table 4) because they were not central in our analysis.

Our classifications revealed that in 1990, 74% of the study area was FA. This FA then decreased to 68% by 2000, but gradually increased again to 77% by 2010. Cropland increased from 1990 to 2000 from 19% to 26%, but decreased again to 19% by 2010. Bare land decreased while built-up area increased from 1990.

Land cover classifications and change across the four counties were very similar across the whole area through the observation period. For example, the FA in Jinping decreased from 80% to 78% at first, then increased to 81%; while cropland increased from 19% to 21% then dropped to 17%. An exception to the overall trends was FA change in Hekou county where the FA percentages in 1990, 2000 and 2010 were 84%, 86% and 82% respectively.

4.2. Reforestation rates and cropland gain or loss

We found interesting patterns in LULCC occurring around growing urban areas, with the expansion of peri-urban zones occurring faster in the east than in the west (Fig. 2). In 1999, ten years before the reforestation programmes, both the strongest variation of Relative Net Change (RNC) of FA and cropland occurred in Maguan (−21%, 105%), followed by Malipo, Jinping, Hekou (Fig. 2a and b). Coincidentally the strongest variation happened in Maguan during 2000 to 2010 with FA 133% and cropland 53%. Transitions between FA and cropland indicate a change of land gain or loss a step further: during 1990–2000 Hekou gained the most FA (106%), while Maguan gained the most cropland (242%).

Variations at the township level were also observed for the FA, cropland disturbance rate and NTR (Fig. 2e1, e2, f1 and f2). The FA disturbance rate occurred faster from east to west before and during the reforestation programmes: the largest FA loss was in Daping in north-western Malipo (−8%) and then during the reforestation programme the largest gain in FA was in Mengqiao in central northern Hekou (8%), followed by the majority of other township areas in Malipo. The largest cropland gain was in the township area of Poqiao, in northern Maguan (30%), while the largest cropland loss was in Miechang, southwest Maguan (−7%). The NTR of FA loss first occurred most strikingly to the west of the study region, while gains in reforestation occurred after 2000 far more to the east of the study region. The NTR of cropland increased the fastest in the township area of Miechang in Maguan (419%) between 1990 and 2000, while township areas to the west experienced more crop conversions from 2000 to 2010, but at a slower rate.

An example of land cover change of cropland increase before reforestation, and FA increase during the reforestation programme in Maguan is shown in Fig. 3. Land cover disturbance rates also revealed the similar strongest variations occurring in Maguan: with FA −2% and cropland 10% (1990–2000); FA 3% and cropland −5% (2000–2010).

The slope of the areas that transitioned from cropland into FA was mostly between 15° and 25° (Fig. 4). While there were no rules regarding specific slope values for conversion in the “Regulations of SLCP” (PRC State Council 2002), an announcement by the State Council on Improving SLCP Policies (PRC State Council 2007) indicated that slopes more than 25° should be targeted (see also Uchida et al., 2005; Weyerhaeuser et al., 2005).

4.3. Urbanization and socioeconomic change

Land cover classification for the four counties and socioeconomic data indicate that there was rapid urbanization (Fig. 5), coupled with population increase and income growth in all four counties since 1990 (Fig. 6). The four head towns experienced urban sprawl during 1990–2000, which then continued to even a greater degree during the reforestation programmes period. Maguan was the most populated county throughout the period, growing from 337,000 to 368,000 people, followed by Jinping, Malipo and Hekou. The percentage of ethnic minorities increased slightly for all counties in the three time staged census (Jinping: from 85% to 86%; Hekou: from 61% to 62%; Maguan: from 49% to 51%; Malipo: from 40% to 42%) (Fig. 6a).

Yunnan statistical yearbook data (Statistical Bureau of Yunnan Province, 1991, 1993, 1995, 1997, 1999, 2001, 2003, 2005, 2007, 2009, 2011) indicated a ten to twenty-times growth of per capita income by county (PCI), and six to twelve times growth of per capita income by rural household (RHI) (Fig. 6b). The highest PCI was Hekou, with an increase from US$179 in 1990 to US$2815 in 2010, contrasting with Jinping that had the lowest income which rose from US$41 to US$889. Maguan recorded the highest RHI in 1992 (US$77). By 2010 this had increased six-fold to US$476. However by 2010 the highest RHI was recorded for Hekou (US$544). The lowest RHI was in Jinping at US$31 in 1992, which rose to US$337 in 2010.

5. Discussion

5.1. Spatial semantic characteristics

Our approach highlighted the regional differences of FA and cropland area over the 1990–2010 period. The inclusion of spatial

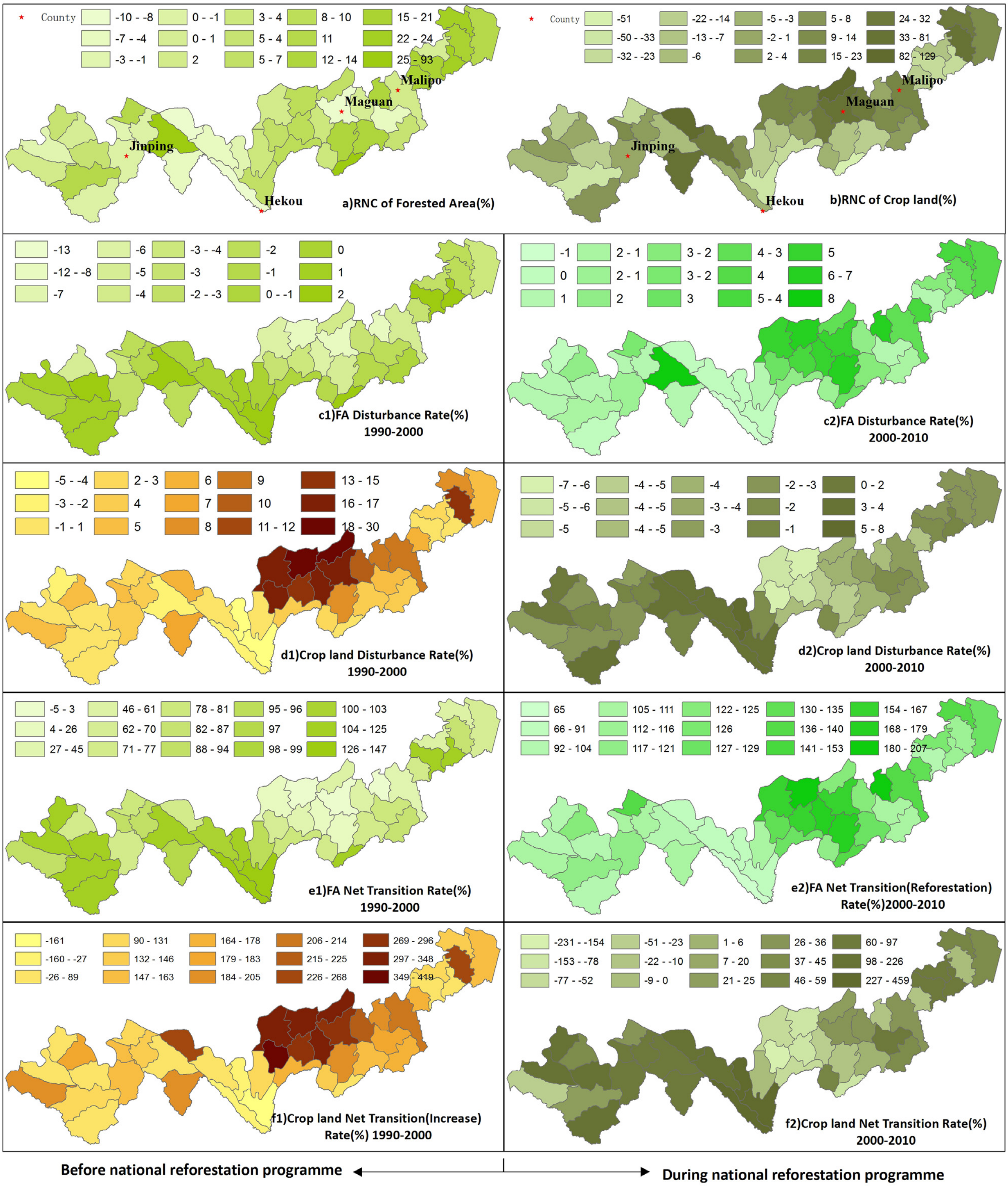

Fig. 2. Land cover change before and during the national reforestation programmes at the township level. (a) Relative net change of FA from 1990 to 2010, (b) Relative net change of cropland from 1990 to 2010, (c) FA disturbance rate, (d) cropland disturbance rate, (e) FA net transition rate, and (f) cropland net transition rate.

semantics in the selection of training points for the classification provided more robustness to cope with uncertainties and helped us to distinguish land cover with similar reflectance to yield classifications with high accuracy.

Notwithstanding the high accuracy achieved by our classifications, errors and uncertainties remain. First, the SSC strategy was predominantly based on expert knowledge and field investigation. To some degree this may increase uncertainties of some unusual relationships which would incur the possibility of incorrect training datasets as mixed pixels. Second, to reduce the similarity of land cover types and distinguish different land use types, secondary detailed categories were added to some small sized classes (e.g. built-up area, bare land) corresponding with intense training points in this region especially around the head towns of counties.

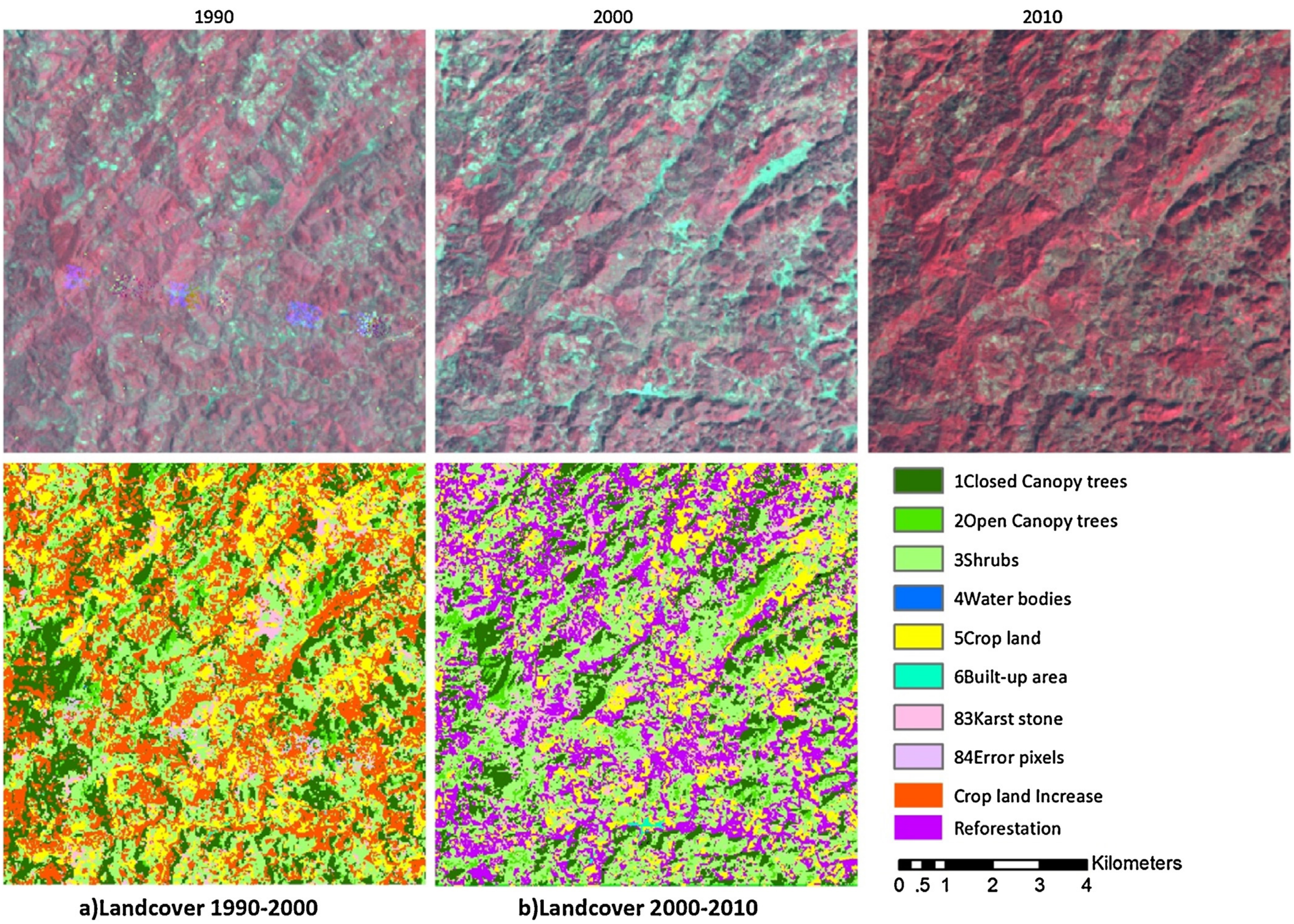

Fig. 3. Example subset of land cover classifications at 9 km × 9 km. This area experienced large cropland increases before the reforestation programmes and then conversion of cropland to FA during the programmes. (a) Predominant land cover change from 1990 to 2000; the base map is the land cover classification of 1990, (b) predominant land cover change from 2000 to 2010; the base map is land cover classification of 2000.

Nevertheless, more categories reduce accuracy levels, e.g. the producer's accuracy for built-up area in 1990 conducted with the ground truth data was as low as 50%. Third, forests in this region are very heterogeneous and it was hard to limit classification types. At the same time, some points were hard to label to the right position at the boundaries (cf. Brandt et al., 2012). These uncertainties or errors may have led to mistakes regarding the overestimation of shrubs or open canopy forest.

The SSC training design was aided by the vegetation index (NDVI), different band composites and other manual comparisons with the images themselves. Yet, uncertainties exist and with different types of vegetation in different seasons in mixed pixels, using this strategy to reduce estimate errors in this region needs to be further explored in future research.

5.2. Forested area and cropland change

Economic reforms since the 1980s and the return of land use rights to households under China's "household responsibility" programme, following the cooperative period, have stimulated agricultural production, land fragmentation and an agrarian transition (Spoor et al., 2007). In combination with the "Western Development Strategy," southeast Yunnan has undergone important land cover changes including urbanization, degradation, reforestation, and agricultural intensification in the past two decades (Hao, 1998; Tong and Nu, 2011). The land use change and livelihood impacts of these initiatives are highly uneven across space, time and ethnic group. The SLCP has been argued to have improved land sustainability and the ecological environment, while also increasing upland farmers' incomes. Yet, studies have also shown that increased farmer incomes have been mainly as a result

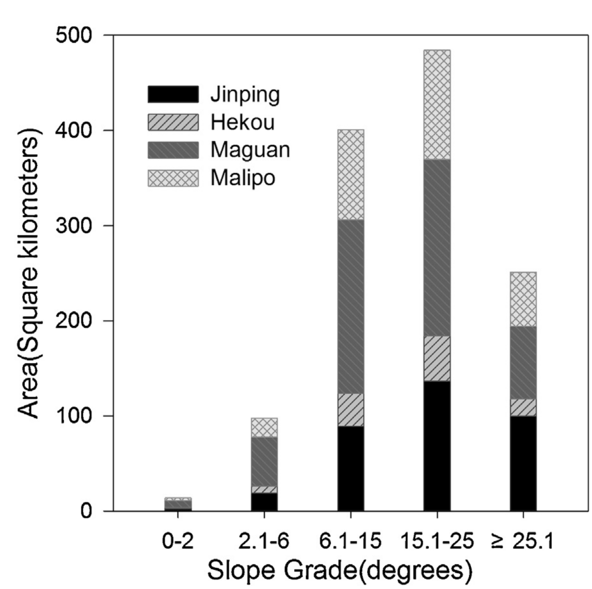

Fig. 4. Conversion of Cropland to Forest and Grassland during 2000–2010.

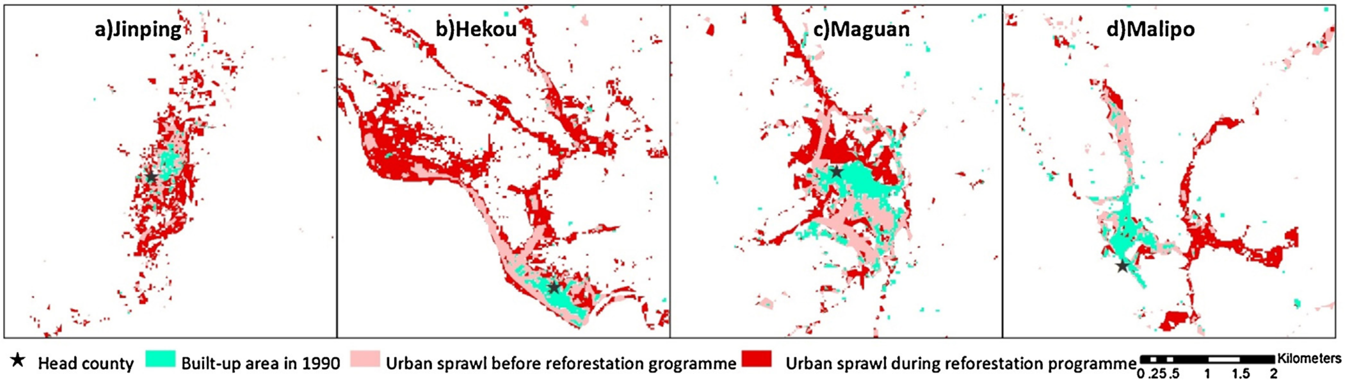

Fig. 5. Urbanization of the four capital counties during 1990–2010 with area of 8 km × 8 km per county.

of government subsidies and after the reforestation programmes, farmers have complained of difficulties in maintaining stable livelihoods (China National Forestry Economics and Development Research Center, 2005; Chen et al., 2006).

From our satellite image classification we interpret that croplands increased 8%, while FA decreased 6% from 1990 to 2000. From 1990, due to population increase and livelihood changes supported by government policies, cropland expanded. Yet, at the same time forest, as well as grass land area, decreased rapidly (Liu et al., 2008). The main form of FA decrease was shrubs occurring near settlements or along rivers and roads. After 2000 the increase in total FA seems to show that reforestation policies that the Chinese government implemented at the beginning of the new millennium to halt transformations from forest to cropland were successful, including the "Returning Grazing Land to Grassland" policy that came into effect in 2003. Following the implementation of the policies, both shrubs and closed canopy forest classes increased.

The average speed and trends regarding land cover change differed little among the four counties. Population density was higher from east to west which may account in part for the

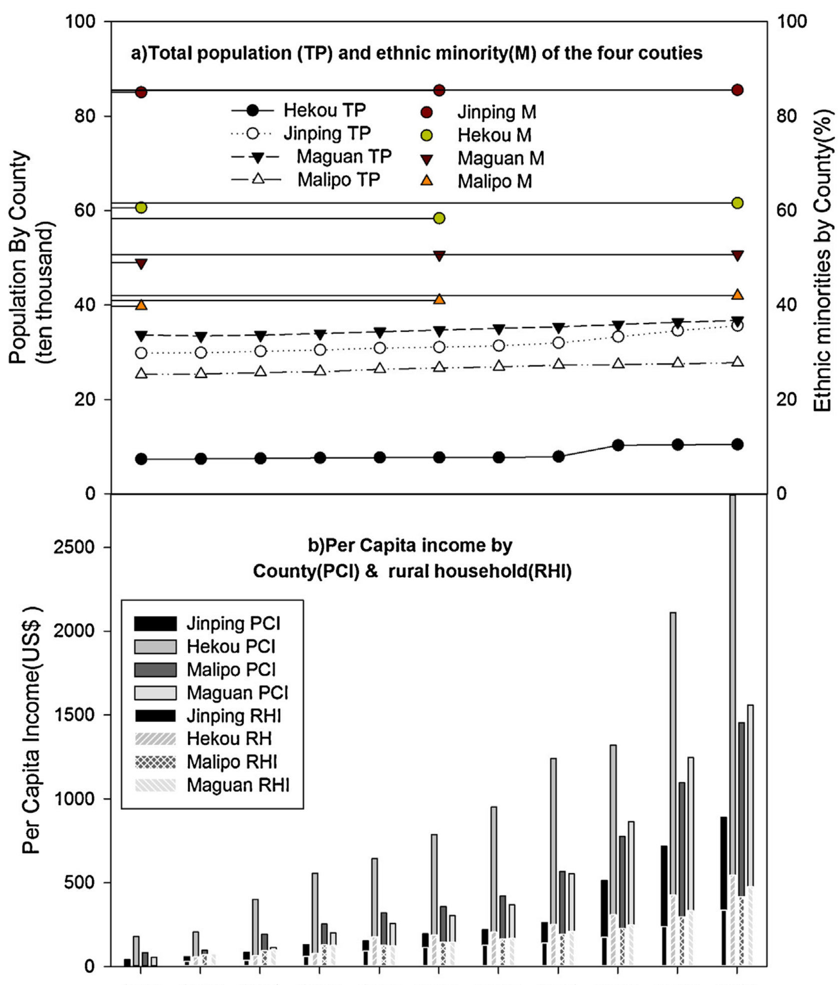

Fig. 6. Population and per capita income by county and rural household during 1990–2010. (US$1 = CNY6.3125 in year 2012). Note: there is a data shortage for RHI in 1990.

differences in spatial distribution. Land cover changes in Maguan were among the fastest. Local policies have no doubt played an important role in this LULCC. During the "Ninth Five-Year" state planning period (1996–2000), Maguan vigorously implemented a "Winter Agriculture" development project. This meant that agricultural land increased from 2247 hectares in 1997 to 7393 hectares in 2000 (Local Chronicle Office of Wenshan Prefecture, 1996, 1997, 1998, 1999, 2000, 2011; Local Chronicle Office of Honghe Prefecture, 1998, 1999, 2005, 2009, 2010). Following this, in the early 2000s, Maguan state policies supported and often subsidized the annual planting of tens of thousands of cash crop plants including flax, *Amomum tsao-ko*, star anise (Pinyin: *bajiao*), pseudo-ginseng (Pinyin: *sanqi*) and tobacco. Returns were severely hampered however, by the significant drought in 2009 and 2010, which hit hardest to the east of the study area. Most recently in 2013, Wenshan prefecture (within which Maguan and Malipo counties are located) received US$7.7 million from the Chinese central government to support the "Comprehensive control project of rocky desertification" (Pinyin: *Shimohua Zonghe Zhili*). This project aims at improving agricultural conditions in the karst area and support for vegetation recovery (Forestry Bureau of Wenshan Prefecture, 2012).

Our results also show that land cover change trends of FA and cropland in Hekou were different from the three other counties. In Hekou, cropland coverage dipped first and then increased. Records for croplands in Hekou are difficult to find, but those that we did recover support our analysis, with a slight increase of cropland from 4104 hectares in 2004 to 5178 hectares in 2008 (Local Chronicle Office of Honghe Prefecture 2005, 2009). The FA trend is opposite, first rising and then declining, with open canopy forest contributing the most to the change over time. We interpret these trends in Hekou in relation to two different elements. First, due to the county being more accessible than the others due to lower altitude and road infrastructure along the Red River, it is likely that afforestation started earlier here, before the year 2000. Second, Hekou has continued to experience important infrastructure development in the past ten years due to its strategic location along a core corridor/transportation route within the Greater Mekong Subregion (Turner, 2013). This has increased urban growth as well as farmer access to subsidies for cash crops, both resulting in local forest decline.

The Go West Campaign was implemented in 2000 (PRC State Council 2000) and southwest China was targeted for additional investment (Niu, 2000). Numerous dam projects were included in the "West-to-east power transmission" strategy and support for other pillar industries: tobacco cultivation, biological resources, minerals and tourism also increased (Li, 2000). Urban growth and road and railway infrastructural development escalated, contributing to a decrease in croplands in peri-urban areas. Nonetheless, to feed an increasing population, croplands have expanded into former forest, grass land, and bare land.

6. Conclusions

In this article we have quantified forest area, cropland, as well as four other land cover types in the southeast borderlands of Yunnan province. Our temporal focus extended from 1990, ten years before widespread state reforestation programmes were initiated, to 2010, which followed a decade of the implementation of the programmes. To complete this quantification, we used spatial semantic characteristics (SSC) combined with other techniques, aided by a SVM classifier to perform land cover classification using Landsat TM images. While historical training data was limited, identifying the land cover patterns using the SSC strategy with domain experts offered the possibility to study forested area and cropland cover changes in a very rugged and diversified region, to highlight these two land cover transitions. Our results suggest that from 1990 to 2000, forest cover decreased while cropland expanded, while from 2000 to 2010 our case study region experienced a small conversion from cropland to forested land. The total forested area observed increased 3% from 1990 to 2010; this matches findings in other regions of southwest China (Brandt et al., 2012).

Within the four county study region, important variations at the county and township levels over time – more noticeable in the east – indicate that socioeconomic conditions as well as local policies and regulations likely influenced forest area and cropland transitions, as suggested to also be the case in other parts of Yunnan (Baumann et al., 2012). While increasing cash crops may be a clever move to change bare land into 'green', for the national (and international) reforestation movement, problems remain. Not only do large mono-crops of cash crops provide limited ecosystem services and diversity, but rubber and tea plantations in this region are suggested to cause soil erosion and serious land degradation (Giertz et al., 2005; Li et al., 2012). The ongoing dilemma remains as to how to protect forested areas while expanding cropland to provide food security and livelihoods for ethnic minority farmers in this region. While the reforestation programmes put into effect in our study region – where we found increased forested areas in the last decade – compensate the loss of forested land cover during 1990–2000, field observations for the east of this region also indicate serious drought, increasing extreme weather events and stony desertification. This draws attention to the importance of scale in such investigations, and that careful attention is needed when creating policies to balance livelihoods and environmental benefits. In sum, the land covers and land uses in these Chinese borderlands are highly complex with diverse patterns across the four study counties. State policies to increase forest cover and improve livelihoods in this region need to consider such diversity with further remote sensing studies such as this, coupled with additional field observations and in-depth qualitative methods.

Acknowledgements

This work was financially supported by the Chinese Scholarship Council (Grant 2010[5013]) to allow Jialong Zhang to be a visiting scholar in the Department of Geography, McGill University, a NSFC (31260156) and National Key Discipline of Forest Management support from Southwest Forestry University (XKZ200901). Thanks to Navin Ramankutty, Jean-François Rousseau and Clara Champalle, Department of Geography, McGill, for helpful discussions and background data; to Jodi Brandt, University of Michigan, for methodology advice; and to Andreas Rabe, Humboldt-Universität, Berlin for accuracy assessment discussions. Thanks also to Cairong Yue and Leiguang Wang in Kunming for critical discussions. Libo Zeng and Chuanping Jin helped collect ground truth data. We thank the anonymous reviewers for their suggestions to improve this manuscript.

References

Baumann, M., Ozdogan, M., Kuemmerle, T., Wendland, K.J., Esipova, E., Radeloff, V.C., 2012. Using the Landsat record to detect forest-cover changes during and after the collapse of the Soviet Union in the temperate zone of European Russia. Remote Sensing of Environment 124, 174–184.

Berk, A., Bernstein, L.S., Anderson, G.P., Acharya, P.K., Robertson, D.C., Chetwynd, J.H., Adler-Golden, S.M., 1998. MODTRAN cloud and multiple scattering upgrades with application to AVIRIS. Remote Sensing of Environment 65, 367–375.

Bonan, G.B., 2008. Forests and climate change: forcings, feedbacks, and the climate benefits of forests. Science 320, 1444–1449.

Brandt, J.S., Kuemmerle, T., Li, H.M., Ren, G.P., Zhu, J.G., Radeloff, V.C., 2012. Using Landsat imagery to map forest change in southwest China in response to the national logging ban and ecotourism development. Remote Sensing of Environment 121, 358–369.

Card, D.H., 1982. Using known map category marginal frequencies to improve estimates of thematic map accuracy. Photogrammetric Engineering and Remote Sensing 48, 431–439.
Chander, G., Markham, B.L., Helder, D.L., 2009. Summary of current radiometric calibration coefficients for Landsat MSS, TM, ETM+, and EO-1 ALI sensors. Remote Sensing of Environment 113, 893–903.
Chen, Z.H., Xu, J., Kang, P.F., 2006. Influence of returning land for farming to forestry on the utilization of upland in Yunnan. Yunnan Geographic Environment Research 18, 20–25.
China National Forestry Economics and Development Research Center, 2005. A Report for Monitoring and Assessment of the Socio-economic Impacts of China's Key Forestry Programs 2004. China Forestry Publishing House, Beijing.
Chowdhury, R.R., Turner, B.L., 2006. Reconciling agency and structure in empirical analysis: smallholder land use in the southern Yucatan, Mexico. Annals of the Association of American Geographers 96, 302–322.
Congalton, R.G., 1991. A review of assessing the accuracy of classifications of remotely sensed data. Remote Sensing of Environment 37, 35–46.
Congalton, R.G.G.K., 2009. Assessing the Accuracy of Remotely Sensed Data Principles and Practices. CRC Press/Taylor & Francis, Boca Raton.
Foley, J.A., DeFries, R., Asner, G.P., Barford, C., Bonan, G., Carpenter, S.R., Chapin, F.S., Coe, M.T., Daily, G.C., Gibbs, H.K., Helkowski, J.H., Holloway, T., Howard, E.A., Kucharik, C.J., Monfreda, C., Patz, J.A., Prentice, I.C., Ramankutty, N., Snyder, P.K., 2005. Global consequences of land use. Science 309, 570–574.
Foody, G.M., 2002. Status of land cover classification accuracy assessment. Remote Sensing of Environment 80, 185–201.
Foody, G.M., Mathur, A., 2004. Toward intelligent training of supervised image classifications: directing training data acquisition for SVM classification. Remote Sensing of Environment 93, 107–117.
Forestry Bureau of Wenshan Prefecture, 2012. Wenshan Prefecture received 48 million RMB in 2012 from the central budget for Comprehensive control project of rocky desertification. http://www.wszly.ynws.gov.cn/research/kgsj/201305/244.html (last accessed: 09.05.13).
Giertz, S., Junge, B., Diekkrüger, B., 2005. Assessing the effects of land use change on soil physical properties and hydrological processes in the sub-humid tropical environment of West Africa. Physics and Chemistry of the Earth, Parts A/B/C 30, 485–496.
Goodman, D.S.G., 2004. China's Campaign to "Open up the West": National, Provincial, and Local Perspectives. Cambridge University Press, Cambridge, New York.
Gray, C.L., Bilsborrow, R.E., Jason, L.B., Lu, F., 2008. Indigenous land use in the Ecuadorian Amazon: a cross-cultural and multilevel analysis. Human Ecology 36, 97–109.
Hao, X.Z., 1998. Yunnan land use sustainable research. Yunnan Geographic Environment Research 10, 81–88.
Jakobsen, J., Rasmussen, K., Leisz, S., Folving, R., Quang, N.V., 2007. The effects of land tenure policy on rural livelihoods and food sufficiency in the upland village of Que, North Central Vietnam. Agricultural Systems 94, 309–319.
Kuemmerle, T., Chaskovskyy, O., Knorn, J., Radeloff, V.C., Kruhlov, I., Keeton, W.S., Hostert, P., 2009. Forest cover change and illegal logging in the Ukrainian Carpathians in the transition period from 1988 to 2007. Remote Sensing of Environment 113, 1194–1207.
Lai, H.H., 2002. China's western development program: its rationale, implementation, and prospects. Modern China 28, 432–466.
Li, H.M., Ma, Y.X., Liu, W.J., Liu, W.J., 2012. Soil changes induced by rubber and tea plantation establishment: comparison with tropical rain forest soil in Xishuangbanna, SW China. Environmental Management 50, 837–848.
Li, Y.H., 2000. Yunnan initiated west-to-east power transmission project. Yunnan Daily (in Chinese), November 6, URL http://www.chinawest.gov.cn/web/NewsInfo.asp?NewsId=20134
Liu, J.G., Li, S.X., Ouyang, Z.Y., Tam, C., Chen, X.D., 2008. Ecological and socioeconomic effects of China's policies for ecosystem services. Proceedings of the National Academy of Sciences of the United States of America 105, 9477–9482.
Local Chronicle Office of Honghe Prefecture, 1998, 1999, 2005, 2009, 2010. Yearbook of Honghe Prefecture. Yunnan People's Publishing House (in Chinese).
Local Chronicle Office of Wenshan Prefecture, 1996, 1997, 1998, 1999, 2000, 2011. Almanac of Wenshan. Dehong Ethnic Press (in Chinese).
Matthew, M.W., Adler-Golden, S.M., Berk, A., Richtsmeier, S.C., Levine, R.Y., Bernstein, L.S., Acharya, P.K., Anderson, G.P., Felde, G.W., Hoke, M.P., Ratkowski, A., Burke, H.H., Kaiser, R.D., Miller, D.P., 2000. Status of atmospheric correction using a MODTRAN4-based algorithm. In: Shen, S.S., Descour, M.R. (Eds.), Algorithms for Multispectral, Hyperspectral, and Ultraspectral Imagery Vi. Spie-Int Soc Optical Engineering, Bellingham, pp. 199–207.
Muller, D., Munroe, D.K., 2008. Changing rural landscapes in Albania: cropland abandonment and forest clearing in the postsocialist transition. Annals of the Association of American Geographers 98, 855–876.
Niu, S.R., 2000. Yunnan: Building the great international passage. China Daily, August 28, (in Chinese). URL http://www.people.com.cn/GB/channel3/21/20000907/222582.html
Olofsson, P., Foody, G.M., Stehman, S.V., Woodcock, C.E., 2013. Making better use of accuracy data in land change studies: estimating accuracy and area and quantifying uncertainty using stratified estimation. Remote Sensing of Environment 129, 122–131.
Peng, Y., 1996. The Politics of Tobacco: relations between farmers and local governments in China's Southwest. The China Journal, 67–82.
Pontius, R.G., 2002. Statistical methods to partition effects of quantity and location during comparison of categorical maps at multiple resolutions. Photogrammetric Engineering And Remote Sensing 68, 1041–1049.
PRC (People's Republic of China) State Council, 2000, October 26. Notice on the Implementation of the Western Development Policy Measures by the State Council Issue No. 2000 [33].
PRC State Council, 2002, December 6. Regulations of Conversion of Cropland to Forest and Grassland. Issue No. 2002 [367].
PRC State Council, 2007. Improving Grain Policies State Council on Sloping Land Conversion Programme Issue No. 2007[25].
Richards, J.A., Jia, X., 1999. Remote Sensing Digital Image Analysis: An Introduction. Springer, Berlin/New York.
Sexton, J.O., Urban, D.L., Donohue, M.J., Song, C., 2013. Long-term land cover dynamics by multi-temporal classification across the Landsat-5 record. Remote Sensing of Environment 128, 246–258.
Singh, A., 2002. Understanding China's 'Go-West' campaign. China Report 38, 121–127.
Song, M., Civco, D.L., Hurd, J.D., 2005. A competitive pixel-object approach for land cover classification. International Journal of Remote Sensing 26, 4981–4997.
Spoor, M., Heerink, N., Qu, F., 2007. Dragons With Clay Feet? Transition, Sustainable Land Use, and Rural Environment in China and Vietnam. Lexington Books, Lanham, MD.
Statistical Bureau of Yunnan Province, 1991, 1993, 1995, 1997, 1999, 2001, 2003, 2005, 2007, 2009, 2011. Yunnan Statistical Yearbook. China Statistics Press (in Chinese).
Stehman, S.V., 2004. A critical evaluation of the normalized error matrix in map accuracy assessment. Photogrammetric Engineering and Remote Sensing 70 (6), 743–751.
Stehman, S.V., Czaplewski, R.L., 1998. Design and analysis for thematic map accuracy assessment: fundamental principles. Remote Sensing of Environment 64 (3), 331–344.
Takada, T., Miyamoto, A., Hasegawa, S.F., 2010. Derivation of a yearly transition probability matrix for land-use dynamics and its applications. Landscape Ecology 25, 561–572.
Ton, J.C., Sticklen, J., Jain, A.K., 1991. Knowledge-based segmentation of Landsat images. IEEE Transactions on Geoscience and Remote Sensing 29, 222–232.
Tong, S.Y., Nu, Y.X., 2011. A study on vertical spatial transfer of cultivated land in Yunnan Province from 1986 to 2008. Agricultural Science & Technology 12, 127–132.
Tortora, R., 1978. A note on sample size estimation for multinomial populations. The American Statistician 32, 100–102.
Turner, S., 2013. Under the state's gaze: upland trading-scapes on the Sino-Vietnamese border. Singapore Journal of Tropical Geography 34, 9–24.
Uchida, E., Xu Jintao, S., Rozelle, 2005. Cost-effectiveness and sustainability of China's conservation set-aside program. Land Economics 81 (2), 247–264.
Vanwambeke, S.O., Lambin, E.F., Eichhorn, M.P., Flasse, S.P., Harbach, R.E., Oskam, L., Somboon, P., van Beers, S., van Benthem, B.H.B., Walton, C., Butlin, R.K., 2007. Impact of land-use change on dengue and malaria in northern Thailand. Ecohealth 4, 37–51.
Wang, J.W., 2012. Building a Green Economy Corridor on the Road Along Honghe Valley Xinhua News (in Chinese), August 22, URL http://www.yn.xinhuanet.com/gov/2012-08/22/c_131799883.htm
Weyerhaeuser, H., Wilkes, A., Kahrl, F., 2005. Local impacts and responses to regional forest conservation and rehabilitation programs in China's northwest Yunnan province. Agricultural Systems 85, 234–253.
Woodcock, C.E., Allen, R., Anderson, M., Belward, A., Bindschadler, R., Cohen, W., Gao, F., Goward, S.N., Helder, D., Helmer, E., Nemani, R., Oreopoulos, L., Schott, J., Thenkabail, P.S., Vermote, E.F., Vogelmann, J., Wulder, M.A., Wynne, R., Team, L.S., 2008. Free access to Landsat imagery. Science 320, 1011-1011.
Wu, S.Y., Shen, M.B., Wang, J.A., 2010. Jinping hydropower project: main technical issues on engineering geology and rock mechanics. Bulletin of Engineering Geology and the Environment 69, 325–332.
Xu, J., Yin, R., Li, Z., Liu, C., 2006. China's ecological rehabilitation: unprecedented efforts, dramatic impacts, and requisite policies. Ecological Economics 57, 595–607.
Xu, Z.G., Bennett, M.T., Tao, R., Xu, J.T., 2004. China's sloping land conversion programme four years on: current situation and pending issues. International Forestry Review 6, 317–326.
Yang, Z.G., 2012. Yunnan produces two new breed varieties of Jatropha Curcas with yield twice higher than old varieties. Yunnan Daily (in Chinese), January 8, URL http://yn.yunnan.cn/html/2012-01/08/content_1989909.htm
Yang, Z.S., Yang, L.F., Zhang, B.S., 2010. Soil erosion and its basic characteristics at Karst Rocky-desertified land consolidation area: a case study at Muzhe Village of Xichou County in Southeast Yunnan, China. Journal of Mountain Science 7, 55–72.
Yunnan Census Office and Statistical Bureau of Yunnan Provincial Government, 2012. Tabulation on the 2010 Population Census of Yunnan province. China Statistics Press, Beijing.